Stereochemical π-Facial Selectivity of the Diels−Alder Reaction of Benz[*a*]aceanthrylene and 1,4-Diphenylbenz[*a*]aceanthrylene

Benjamin F. Plummer,* Saadia Faiz, Ted Wiederhold, Marilyn Wooten, and Joseph K. Agyin

Department of Chemistry, Trinity University, San Antonio, Texas 78212

Kurt L. Krause and Mitchell D. Miller

Department of Biochemistry and Biophysical Sciences, University of Houston, Houston, Texas 77204-5934

William H. Watson

Department of Chemistry, Texas Christian University, Fort Worth, Texas 76129

Received August 28, 1997[⊗]

The Diels−Alder (D−A) reaction of the twisted hydrocarbon 1,4-diphenylbenz[*a*]aceanthrylene (**4**) with dienophiles maleic anhydride, bromomaleic anhydride, and *N*-phenylmaleimide and with benzyne is reported. The stereochemistry of the products derived from the D−A reaction of **4** is compared with the products derived from reaction of planar benz[*a*]aceanthrylene (**5**) with maleic anhydride as a model. The *endo* regiochemical π-facial selectivity of **4** appears to be the result of the steric effect of a phenyl substituent as the transition state is reached. Compound **5** produces both *endo* and *exo* D−A adducts when treated with maleic anhydride. X-ray crystallographic analysis verifies the topology of the bromomaleic anhydride adduct of **4** and the maleic anhydride adduct of **5**.

The objective of this study is to characterize the π-facial diastereoselectivity that determines the products that result from the reaction of the dienophiles maleic anhydride (**1**), bromomaleic anhydride (**2**), and *N*-phenylmaleimide (**3**) with the distorted hydrocarbon 1,4-diphenylbenz[*a*]aceanthrylene (**4**).[1−3] The regioselectivity of the reaction of **2** with **4** is also identified. The Diels−Alder reaction of **1** with the planar parent hydrocarbon benz[*a*]aceanthrylene (**5**) is studied to compare the effects of the phenyl substituents on the stereochemistry of the products derived from **4**.[1,4] Facial selectivity in Diels−Alder (D−A) reactions continues to stimulate widespread interest.[5,6] We wondered if the anthracene core, whose molecular orbitals are perturbed by fusion to ring B in **4**, would exhibit reactivity similar to that of anthracene (**6**) itself. We have discovered that **4** and **5** exhibit interesting photochemistry,[7] and we wanted to see if their ground-state Diels−Alder reactions would occur at the "meso" positions of the anthracene moiety as observed for **6**.[8]

Results and Discussion

Molecular mechanics calculations predict and X-ray analysis verifies that the geometry of **4** has a pronounced twist of the rings ABC out of the *zy* plane relative to the rings DEF (anthracene core) (Figure 1). The phenyl substituents in **4** cause distortion of the polycyclic aromatic hydrocarbon (PAH) from planarity[9,10] as modeled by the ball-and-stick figure. This distortion induces chirality, and the X-ray analysis of crystalline **4** could not be resolved to high resolution because of the disorder in the crystal lattice. However, the coordinates of the

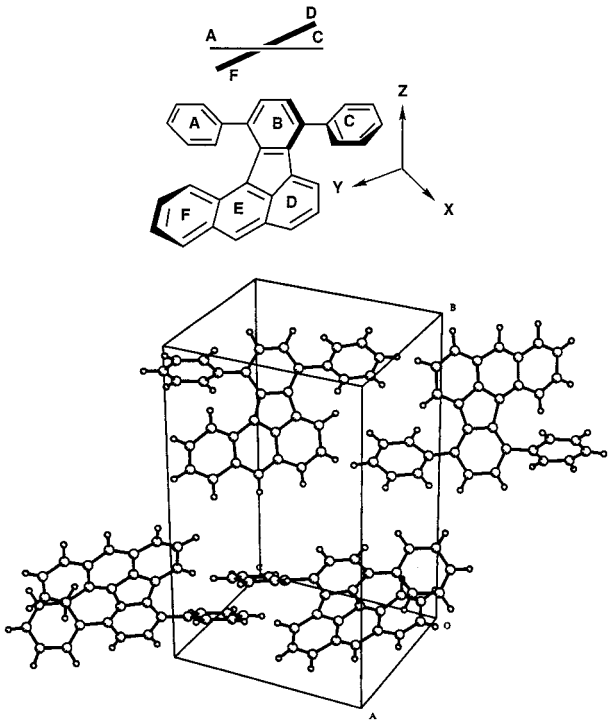

Figure 1. Illustration of distortion from planarity observed in **4**. The terphenyl group ABC is twisted by a steric effect relative to the anthracene moiety DEF as shown in the overlapping line segments AC and DF. A unit cell from X-ray diffraction data is shown.

[⊗] Abstract published in *Advance ACS Abstracts,* December 1, 1997.

(1) Chung, Y.-S.; Kruk, H.; Barizo, O. M.; Katz, M.; Lee-Ruff, E. *J. Org. Chem.* **1987**, *52*, 1284−1288.
(2) Cho, B. P.; Harvey, R. G. *J. Org. Chem.* **1987**, *52*, 5668−5678.
(3) We define the structure with the anhydride moiety lying over the cyclopentene-fused benzo ring as the *endo* adduct.
(4) Plummer, B. F.; Guterriez, S.; Navikov, A.; Goodman, D. *Synth. Commun.* **1997**, *27*, 3213−3217.
(5) Bach, R. D.; McDouall, J. J. W.; Schlegel, H. B. *J. Org. Chem.* **1989**, *54*, 2931−2935.
(6) Mataka, S.; Ma, J.; Thiemann, T.; Rudzinski, J. M.; Sawada, T.; Tashiro, M. *Tetrahedron Lett.* **1995**, *36*, 6105−6106.
(7) Faiz, S. Senior Honor Thesis, Trinity University, 1995.
(8) March, J. *Advanced Organic Chemistry*; Wiley: New York, 1992.
(9) Gilbert, K. E.; Serena Software: Bloomington, IN.
(10) Pindur, U.; Otto, C.; Molinier, M.; Massa, W. *Helv. Chim. Acta* **1991**, *74*, 727−738.

S0022-3263(97)01610-1 CCC: $14.00

Table 1. Calculated Heats of Formation of D−A Adducts Using PCModel

compound	**7a**	**7b**	**7c**	**8a**	**8b**	**8c**
H_f (kcal/mol)	42.8	41.7	46.4	50.0	49.4	49.1

carbon atoms are found to yield a structure that is very similar to that predicted from molecular mechanics calculations. The disorder in the crystal lattice of **4** suggests that puckered conformers unrelated by any symmetry operation behave as acentric molecules which have not crystallized out as a racemic compound. The sterically induced twist leads to conformationally mobile enantiomeric forms which rapidly interconvert in solution. The enantiomeric conformers of **4** in solution are trapped equally in the Diels−Alder reaction with dienophiles and are expected to lead to the production of racemic mixtures of the diastereomers.

When **4** is treated with the dieneophiles **1**, **2**, and **3** by reaction in refluxing toluene, crystalline products are readily isolated. In every case, NMR and TLC examination verified that greater than 95% of the isolated material was a single diastereomer. The possible structures that can result from the dienophiles reacting with **4** are shown (eq 1). Unsymmetrical dienophiles can add to the "meso" positions of **4** in four distinct ways to form the various stereoisomers. When **2** is the dienophile, two regioisomers are possible in which Br and H are interchangeable for Z and Y in **7** and **8**.

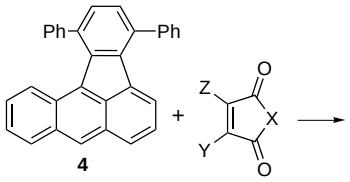

4

1: Y = Z = H, X = O
2: Y = H, Z = Br, X = O
3: Y =Z = H, X = *N*-Ph

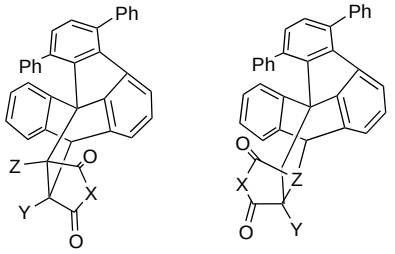

(1)

endo *exo*

7a: Z = Y = H, X = O
7b: Z = H, Y = Br, X = O
7c: Z = Br, Y = H, X = O
7d: Z = Y = H, X = *N*-Ph

8a: Z = Y = H, X = O
8b: Z = H, Y = Br, X = O
8c: Z = Br, Y = H, X = O
8d: Z = Y = H, X = *N*-Ph

We performed a molecular mechanics analysis[9] of the heats of formation of all possible stereoisomers derived from reaction of **1** and **2** with **4** to yield structures **7a**−**c** and **8a**−**c**. In Table 1 the results of the calculation show that the *endo* adducts **7a** and **7b** exhibit the lowest calculated heats of formation. On the assumption that the transition state for an exothermic reaction lies along the reaction coordinate near the reactants as predicted by the Hammond Postulate,[11] we assigned the geometry of the favored diastereomer to the *endo* form based on steric effects. In all cases, racemic mixtures are expected because of the achiral substrate. The ^{1}H NMR spectrum of **7b** readily verified that the bromine substituent occupied position Y as shown. The bridgehead hydrogens

(11) Hammond, G. S. *J. Am. Chem. Soc.* **1955**, *77*, 334−338.

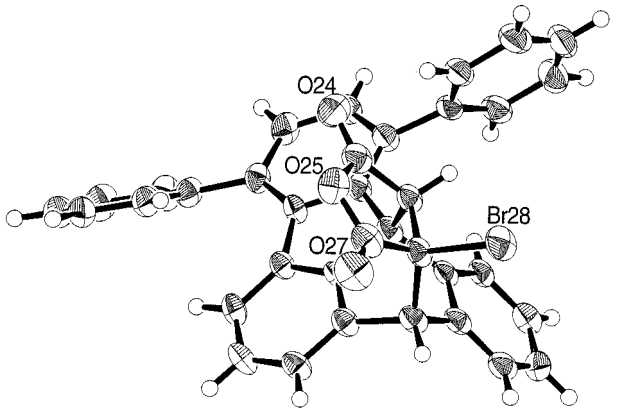

Figure 2. X-ray crystal structure of the adduct **7b** showing the *endo* geometry.

at Z and on the anthracene core appeared as separated singlets at $\delta = 4.1$ and 5.0 indicating that they were not vicinally coupled to each other as they would be in **7c** and **8c**. However, the *endo* or *exo* stereochemistry of the products was difficult to assign on the basis of the NMR results. Crystals of satisfactory quality were obtained upon slow evaporation of a supersaturated solution of **7b** in ethyl acetate and subjected to X-ray crystallographic analysis. The X-ray structure (Figure 2) verifies our initial assumption that the geometry of the adduct is *endo*. The transition state for the formation of **7b** requires that the anthracene moiety begin to fold significantly across the "meso" positions of the anthracene core. The phenyl substituent (C) is relatively unencumbered and can be expected to adopt a variety of conformational geometries during the attack of the dienophile.[12] Phenyl substituent (A) is considerably more hindered and probably encounters higher energy conformational barriers to its rotation.[12] As the dienophile attacks the meso positions of ring E, ring B must twist such that ring A moves toward the dienophile during the attack. The phenyl substituent introduces a significant steric impediment as the transition state is reached. This movement favors regiospecific attack of the dienophile to form the *endo* product. In Table 1 all *exo* adducts are shown by calculation to have higher positive heats of formation relative to their *endo* isomers and this probably reflects the steric effect between ring A and the steric bulk of the dienophile adduct. This same steric effect is assumed to manifest itself in the transition state during the formation of all of the products. Given the similarity in structure of the other dienophiles, we are confident that the adducts **7a**, **7b**, and **7d** have the *endo* geometry.

In the molecular orbital illustration (Figure 3), the HOMO and LUMO of **4** is presented along with selected geometric arrangements of the skeleton of **2** showing its HOMO−LUMO orbitals. It is expected that the HOMO of **4** and the LUMO of **2**, represented on the left of the diagram, would generate the more favorable transition state interaction because the ionization potential (IP) of **4** is expected to be lower than the IP of **2**. The magnitudes of the orbital coefficients in the LUMO of **2** and the HOMO of **4** at the bonding sites in the transition states suggest that orbital overlap does not confer significant π-facial stereoselectivity. The wave function symmetry for good overlap can be appropriately main-

(12) Plummer, B. F.; Steffen, L. K.; Braley, T. L.; Reese, W. G.; Zych, K.; Van Dyke, G.; Tulley, B. *J. Am. Chem. Soc.* **1993**, *115*, 11542−11551.

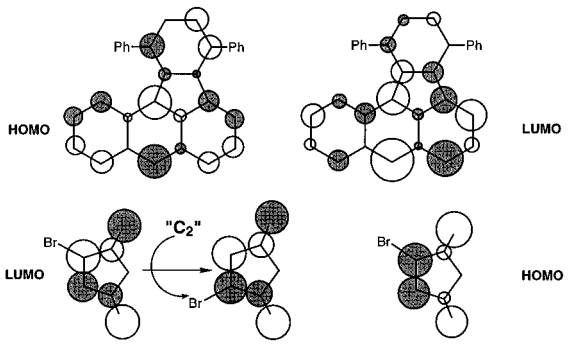

Figure 3. Molecular orbitals of diene and dienophile drawn with the diameter of the circles proportional to the magnitude of the calculated atomic orbital coefficients.

tained in all of the various regiochemical approaches as **2** and **4** join together. For example, if the MOs for the LUMO of **2** as shown are rotated 180° by a C_2 operation (neglecting the dissymmetry introduced by the bromine atom), we see that the frontier orbitals are still of correct symmetry for bond formation. Thus, the frontier orbitals have a significant impact on reaction at the "meso" positions but appear to be of minor consequence in the formation of *endo* and *exo* products formed from reactions of sterically encumbered **4**.[13,14] Small secondary orbital effects resulting from the overlap of dienophile orbitals with those of **4** are likely of minor significance as well.[5,6,10]

When **4** was treated with a mixture of equimolar quantities of **1** and **2** in refluxing toluene, analysis of the reaction mixture proved that **7a** was present and **7b** was absent. We surmise that the steric effect of the bromine considerably slows down the D−A reaction of **2** and offsets any accelerating electronic effect that the bromine substituent might exert. Reflux of pure **7b** in toluene for 10 h showed no change in the composition, suggesting that reversible reaction was not occurring under our experimental conditions and that bromine was not lost from the adduct.

Compound **5**[4] was treated with **1** in refluxing toluene and the *endo* (**9**) and *exo* (**10**) products were formed in a 2:3 ratio (eq 2). The NMR spectrum of the anthracene

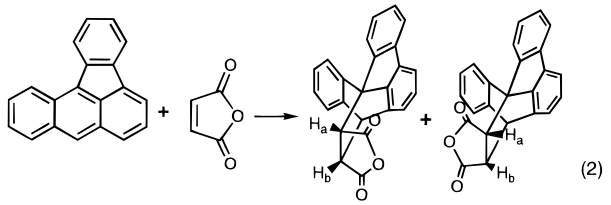

(2)

5 **1** **9** **10**

adduct **12** (eq 3) was chosen as a model. The NMR spectrum of **12** shows a consistent pattern of chemical shifts for selected protons when compared with that of **9**, **10**, and **7b**. In **12** the bridgehead hydrogens H_c exhibit resonances at $\delta = 4.8$ while protons H_a are found at $\delta = 3.5$. Protons in environments similar to H_c in **9**, **10**, and **7b** are chemically shifted to $\delta = 5.06$, 5.02. and 4.9, respectively. Protons H_b in **9** and **10**, and at position Y in **7b**, have chemical shifts of $\delta = 3.62$, 3.75, and 3.70 similar to that for H_a ($d = 3.5$) in **12**. Proton H_a in **10**

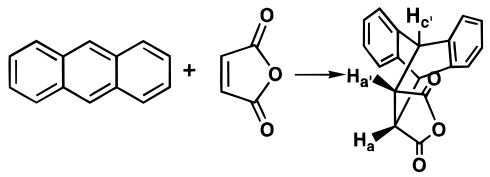

6 **1** **12** (3)

resonates at $\delta = 3.17$ and is shifted upfield relative to H_a in **12**. The upfield shift of H_a, located in the bay region of *exo*-**10** above the benzo substituent, is attributed to the diamagnetic ring current of the adjacent benzo-fused ring. The shift of H_a in *endo*-**9** at $\delta = 3.62$ is consistent with the chemical shift of $\delta = 4.0$ at position Y in **7b** which exhibits additional deshielding caused by the proximate phenyl substituent.

Benzo fusion in **5** thus exerts a small effect upon the formation of the adducts **9** and **10** (eq 2). The result of secondary orbital interactions on the D−A facial selectivity (eq 2) and the possible steric effect of the benzo-fused ring seem to constitute small energy perturbations that are difficult to separate. We assume that the product distribution favors the *exo* isomer because of a small repulsive steric effect caused by the benzo fusion.

Compound **10**, upon slow recrystallization from ethyl acetate, afforded crystals that gave satisfactory X-ray diffraction. It is satisfying to note that our intial *exo* assignment based upon NMR analysis is corroborated by the X-ray structure of **10** (Figure 4). The calculated heats of formation from molecular mechanics calculations for **9** and **10** are identical (−6.7 kcal/mol). The product ratio of 60% of **10** and 40% for **9** in the crude mixture reflects a very small energy difference in the transition state and indicates that π-facial diastereoselectivity is minor. This ratio remains relatively invariant throughout the course of the reaction. It appears that the transition state for the formation of *exo* **10** is slightly favored because of weak repulsive interactions (steric effect) between the maleic anhydride dienophile and the benzo-fused ring. Secondary orbital interactions (electronic effect) are presumed to be small and nearly the same for the transition states leading to **9** and **10**.

Compound **4** reacts readily with the benzyne **(13)** generated from anthranilic acid by aprotic diazotization to produce the triptycene derivative **14** (eq 4).[15,16] The

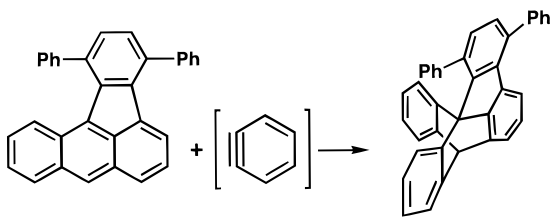

(4)

4 **13** **14**

reaction proceeded smoothly, further corroborating that the anthracene core of **4** maintains signficant reactivity at the "meso" positions for ground-state reactions. We shall report in the future the excited-state reactions of **4** and **5**.

(13) Fringuelli, F.; Taticchi, A. *Dienes in the Diels−Alder Reaction*; Wiley: New York, 1990.
(14) Fleming, I. *Frontier Orbitals and Organic Chemical Reactions*; Wiley: New York, 1976.
(15) Wittig, G.; Niethammer, K. *Chem. Ber.* **1960**, *93*, 944−950.
(16) Dougherty, C. M.; Baumgarten, R. L.; Sweeney, A., Jr.; Concepcion, E. *J. Chem. Educ.* **1977**, *54*, 643−644.

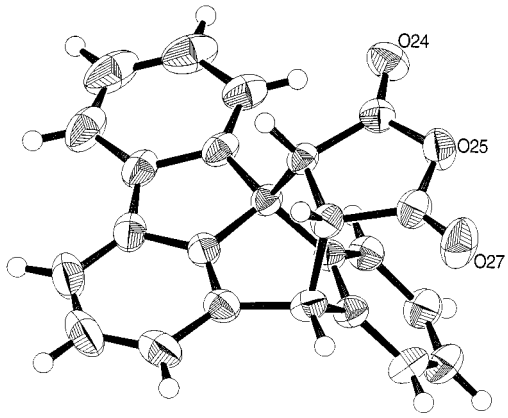

Figure 4. X-ray crystal structure of the adduct **10** showing the *exo* geometry.

Experimental Section

General. ^{1}H NMR spectra were obtained either on a Varian Inova 400 or VXR 300 MHz spectrometer, using $CDCl_3$ solutions, and calibrated on residual $CHCl_3$. Melting points were determined on a Meltemp apparatus and are uncorrected. IR spectra were obtained as KBr pellets on a Nicollet FT-IR. Elemental analyses were performed by Texas Analytical Laboratories. TLC (Whatman, Silica) (70% toluene; 30% hexane) was used to monitor the reactions. All reactions were run in standard taper glassware using a reflux condenser.

1,4-Diphenyl-8,12b-dihydro-8,12b-ethanobenz[*a*]aceanthrylene-*endo*-13,14-dicarboxylic Acid Anhydride (7a). A solution of 20.0 mg (0.049 mmol) of **4**, 57.2 mg (0.581 mmol) of **1**, and 500 μL of toluene was refluxed for 4 h. Impure **7a** crystallized from the cooled solution and was recrystallized from ethyl acetate, rinsed with cold hexane, and dried to give 15.4 mg (61%) of **7a**: mp 244 °C dec; ^{1}H NMR ($CDCl_3$) δ 7.82 (d, 2H, J = 8.34 Hz), 7.38 (m, 12 H), 7.21 (d, 1 H, J = 7.3 Hz), 7.01 (m, 3 H) 6.66 (d, 1H, J = 7.9 Hz), 4.91 (d, 1H, J = 3.7 Hz), 4.00 (d, 1H, J = 9.0 Hz), 3.71 (dd, 1H, J = 9.0,3.7 Hz) ppm; IR (KBr) 2980, 2352, 1863, 1842, 1827, 1769, 1685, 1649, 1560, 1378 cm^{-1}. Anal. Calcd for $C_{36}H_{22}O_3$: C, 85.98; H, 4.41. Found: C, 85.57; H, 4.47.

1,4-Diphenyl-14-bromo-8,12b-dihydro-8,12b-ethanobenz-[*a*]aceanthrylene-*endo*-13,14-dicarboxylic Acid Anhydride (7b). A solution of 21.2 mg (0.052 mmol) of **4**, 61.0 mg (0.345 mmol) of **2**, and 500 μL of toluene was heated to reflux for 10 h. The crude solid was isolated by vacuum filtration and subjected to column chromatography on silica gel with hexane as the eluent to produce 17 mg of **7b** (56%) after isolation by vacuum rotary evaporation: mp 218 °C dec; ^{1}H NMR ($CDCl_3$) δ 4. 1 (s, 1H), 5.0 (s, 1H), 6.7 (d, 2H, J = 7.93 Hz), 7.25 (m, 15 H), 7.8 (d, 2H, J = 7.02 Hz) ppm; IR (KBr) 2980, 2371, 2350, 1865, 1844, 1791, 1718, 1654, 1560, 1508, 1458, 1383, 1262 cm^{-1}. Anal. Calcd for $C_{36}H_{21}BrO_3$: C, 74.30; H, 3.58; Br, 13.87. Found: C, 74.18; H, 4.19; Br, 13.41.

***N*,1,4-Triphenyl- 8,12b-dihydro-8,12b-ethanobenz[*a*]-aceanthrylene-*endo*-13,14-dicarboximide (7d).** A mixture of 25.0 mg (0.062 mmol) of **4**, 65 mg (0.37 mmol) of **3**, and 600 μL of toluene was heated to reflux for 15 h. The adduct crystallized out of solution, isolated by vacuum filtration, and rinsed with ethanol to give 17 mg of **7d** (47%): mp 63−65 °C; ^{1}H NMR ($CDCl_3$) δ 3.57 (dd, 1H, J = 8.3,3.67), 3.9 (d, 1H, J = 8.3), 5.0 (d, 1H, J = 3.66), 6.56 (q, 2H, J = 4.04, 3.59, 1.6), 6.7 (d, 1H, J = 7.87), 6.88 (s, 5H), 7.1 (m, 3H), 7.2 (d, 1H, J = 7.26), 7.3−7.5 (m, 10 H), 7.92 (d, 2H, J = 7.08) ppm; IR (KBr) 3063, 2912, 2840, 1776, 1715, 1505, 1402, 1146 cm^{-1}. Anal. Calcd for $C_{42}H_{27}NO_2$: C, 85.30; H, 4.60; N, 2.37. Found: C, 85.43; H, 4.86; N, 2.41.

1,4-Diphenyl-8,12b-dihydro-8,12b-*o*-phenylenobenz[*a*]-aceanthrylene (14). To a 50 mL round-bottom flask equipped with reflux condenser were added 15 mL of glyme and 105 mg (0.26 mmol) of **4**. The mixture was heated to reflux and upon cooling, anthranilic acid (45 mg, 0.328 mmol) dissolved in 10 mL of glyme, was added followed immediately by the addition of 0.06 mL (0.33 mmol) of isoamyl nitrite. The mixture was refluxed for 1 h and then cooled to 0 °C for 24 h. The resulting small, yellow crystals were isolated by vacuum filtration and washed repeatedly with hexane to give 30 mg of **12** (12%): mp 298−300 °C; ^{1}H NMR ($CDCl_3$) δ 7.94 (2H, m), 7.84 (1H,d, J = 6.9 Hz); 7.53 (1 H, d, J = 8.1 Hz), 7.46 (8 H, m), 7.25 (2 H, m), 7.15 (1H, d, J = 7.0 Hz), 6.96 (4H, m), 6.7 (3H, m), 6.39 (1H, dd, J = 7.4 Hz), 5.55 (1H, s); IR (KBr) 3056, 2960, 1632, 1597, 1439, 828, 767, 697 cm^{-1}. Anal. Calcd for $C_{42}H_{24}$: C, 94.30; H, 5.70. Found: C, 94.18; H, 5.80.

8,12b-Dihydro-8,12b-ethanobenz[*a*]aceanthrylene-*endo*-13,14-dicarboxylic Acid Anhydride (9 and *exo*-10). A mixture of **5** (75 mg, 0.3 mM) and **1** (175 mg, 1.8 mM) was refluxed in 2 mL of toluene for 3 h. The solution was cooled to room temperature, and 3 mL of hexanes was added. The precipitate was recovered by filtration to afford 97 mg (92%) of crude product. TLC indicated a 2:3 mixture (NMR) of two isomers (R_f **10** = 0.24; **9** = 0.13 in 40% ethyl ether, 60% hexanes). Separation of the two products was achieved by radial chromatography on silica gel (hexane, ethyl acetate gradient). Compound **10**: mp 238−240 °C; ^{1}H NMR ($CDCl_3$) δ 8.42 (m, 1H), 7.82 (m, 1H), 7.56 (m, 3H), 7.45 (m, 2H), 7.37 (m, 2H), 7.17 (m, 2H), 5.02 (d, J = 2.75 Hz, 1 H), 3.75 (dd, J = 9.12, 2.77 Hz, 1 H), 3.18 (d, J = 9.12, 1 H); IR (KBr) 2980, 1798, 1378 cm^{-1}. Anal. Calcd for $C_{24}H_{14}O_3$: C, 82.27; H, 4.03; O, 13.70. Found: C, 82.23; H, 4.18. Compound **9**: mp 218−220 °C; ^{1}H NMR ($CDCl_3$) δ 8.83 (m, 2H), 7.61−7.51 (m, 2H), 7.45−7.18 (m, 4H), 5.02 (d, J = 2.75 Hz, 1H), 3.75 (dd, J = 9.12 Hz, 2.77 Hz, 1H), 3.17 (d, J = 9.12, 1H); IR (KBr) 2981, 1797, 1376 cm^{-1}.

Crystallography. Single crystals of **7b** and **10** were obtained by slow evaporation from a saturated solution of ethyl acetate. In both examples enantiomeric forms were also identified in the crystal lattice. Crystals of **4** were obtained by slow evaporation of a hexane solution. Because of the disorder in the crystal lattice of **4**, resolution to high accuracy could not be achieved. For compound **4**, an orange prismatic crystal having approximate dimensions of 0.20 × 0.15 × 0.40 mm was mounted on a glass fiber and analyzed on a Rigaku AFC6S diffractometer with graphite monochromated Cu Kα radiation. Data were collected using the $\omega-2\theta$ scan mode ($3 < 2\theta < 158.6°$) with a scan rate of 8° per minute and multiple scans for weak reflections. Data were corrected for Lorentz and polarization effects, and a Ψ-scan based empirical absorption correction was applied. The function minimized was $\Sigma w(|F_o| - |F_c|)|^2$, where $w = 4F_o^2\sigma^{-2}(F_o^2)^{-1}$. For $C_{32}H_{20}$ the monoclinic space group was $P2_1$ with a = 10.568 (8), b = 17.976 (7), and c = 11.166 (6) Å, V = 2113(4) Å^3, Z = 4, d_{calc} = 1.271 g cm^{-3}, and μ = 5.12 cm^{-1}. A total of 6127 reflections were collected. The structure was solved by direct methods, and the non-hydrogen atoms were refined with anisotropic thermal parameters with H atoms allowed to ride on the attached carbon atoms. The final cycle of full-matrix least-squares refinement was based on 2152 observed reflections ($I > 2.00\sigma(I)$) with 577 variable parameters with convergence to R = 0.08 and wR = 0.074. The goodness of fit was 2.68, the final shift/error = 6.59, and the largest peaks in the final difference map were +0.30 and −0.24 e$^-$/Å^3.

A yellow, plate crystal of **7b** dimension 0.40 × 0.40 × 0.12 mm was mounted on a glass fiber and diffracted at 223(2) K on a Nicolet R3m/V diffractometer using graphite-monochromated Mo Kα radiation. The space group of this $C_{36}H_{21}BrO_3$ crystal was $P\bar{1}$ with a = 9.560(2), b = 11.341(2), and c = 13.533(2) Å, α = 114.48(1)°, β = 98.69(1)°, and γ = 97.62(1)°. Other crystal parameters were cell volume = 1288.6(5) Å^3, Z = 2, d_{calc} = 1.50 g cm^{-3}, and μ = 16.4 cm^{-1}. A total of 4380 reflections were collected using an $\omega - 2\theta$ scan mode to a maximum 2θ value of 50.1°. Reflections were corrected for Lorentz and polarization effects, and a Ψ-scan based empirical absorption correction was applied. The structure determination was accomplished using heavy-atom Patterson methods and expanded using Fourier techniques. In refinement the function minimized was $\Sigma w(F_o^2 - F_c^2)^2$ with a weighting scheme of $w = 1/[\sigma^2(F_o^2) + (0.0638P)^2 + 1.0658P]$, where $P = [2F_o^2 + \mathrm{MAX}(F_o^2, 0)]/3$. Non-hydrogen atoms were refined anisotropically. Hydrogen atoms were included but not re-

fined. The final cycle of full-matrix least-squares refinement was based on all 3480 reflections with 361 variable parameters which converged to $R = 0.0871$ with $R = 0.0528$ for the 3124 reflections with ($F_o^2 > 2\sigma(F_o^2)$). The goodness of fit on F^2 was 1.057 and the final shift/error = 0.00. The peaks of greatest magnitude in the final difference map were +0.74 and −0.58 $e^-/Å^3$.

A clear, prism crystal of **10**, dimension 0.8 × 0.5 × 0.1 mm, was mounted on a glass fiber and diffracted at 288(2) K on a Rigaku AFC5R diffractometer using graphite-monochromated Cu Kα radiation. The space group of this $C_{24}H_{14}O_3$ crystal was $P\bar{1}$ with $a = 10.0205(8)$ Å, $b = 10.8786(6)$ Å, $c = 8.3722(6)$ Å, $\alpha = 90.985(6)°$, $\beta = 113.729(5)°$, and $\gamma = 95.956(6)°$. Other crystal parameters were cell volume = 829.24(10) $Å^3$, $Z = 2$, $d_{calc} = 1.403$ g cm^{-3}, $\mu = 7.43$ cm^{-1}. A total of 2656 observations of 2490 unique reflections were collected using an $\omega-2\theta$ scan mode to a maximum 2θ value of 120.3°. Reflections were corrected for Lorentz and polarization effects, a Ψ-scan based empirical absorption correction was applied, and a secondary extinction was fit. The structure determination was accomplished using direct methods. In refinement, the function minimized was $\Sigma w(F_o^2 - F_c^2)^2$ with weighting scheme of $w = 1/[\sigma^2(F_o^2) + (0.0522P)^2 + 0.2224P]$, where $P = [2F_o^2 + \mathrm{MAX}(F_o^2, 0)]/3$. Non-hydrogen atoms were refined anisotropically. Hydrogen atoms were included but not refined. The final cycle of full-matrix least-squares refinement was based on all 2490 reflections with 245 variable parameters which converged to $R = 0.0377$ and $R = 0.0353$ for the 3124 reflections with ($F_o^2 > 2\sigma(F_o^2)$). The goodness of fit on F^2 was 1.070 and the final shift/error = 0.00. The peaks of greatest magnitude in the final difference map were +0.17 and −0.15 $e^-/Å^3$.

Acknowledgment. We sincerely appreciate the support of NSF Grant CHE-924324,952840, REU Grant NSF CHE 9300130, The Robert A. Welch Foundation, and the W. M. Keck Foundation.

Supporting Information Available: Six NMR spectra and complete X-ray crystallographic details for compounds **7b** and **10** (20 pages). This material is contained in libraries on microfiche, immediately follows this article in the microfilm version of the journal, and can be ordered from the ACS; see any current masthead page for ordering information.

JO971610T